

THERMAL AND ELECTRICAL CONDUCTIVITIES OF GREEN RIVER OIL SHALES*

J. DuBow, R. Nottenburg, and G. Collins

Department of Electrical Engineering
Colorado State University
Fort Collins, Colorado 80523

INTRODUCTION

Oil-shale retorting is a thermal process, yet the thermal conductivity of oil shale is incompletely known.⁽¹⁾ A detailed knowledge of the thermal conductivity is necessary before the temperature distributions in oil-shale rocks, in oil-shale beds, and in the rock surrounding in situ oil-shale retorts may be accurately determined. The limited experimental data and limited theoretical understanding of the thermal conductivity of oil shale to date hinders control of in situ retorting processes and limits the accuracy of mathematical simulations of oil-shale retorting.

Previous studies^(2,3) of the thermal conductivity of oil shale recognized that thermal conductivity could vary with temperature, kerogen content, and varve geometry. However, other aspects of the thermal conductivity were never extensively studied. For example, Prats and O'Brien⁽²⁾ report chemical analyses of oil-shale samples of nearly equal Fischer assay, but which exhibit substantially different mineral matrix compositions. It is unreasonable to expect two oil-shale samples of equal grade but different mineral composition would exhibit identical thermal and electrical conductivities during retorting. Cook⁽⁴⁾ noted that carbonate minerals, such as nahcolite and dawsonite, decomposed over the temperature range used in their experiments and are therefore the most likely minerals to affect the thermal and electrical properties of oil shale. These studies^(2,3) utilized the transient line probe technique to measure thermal conductivity. This technique relies on a diffusional heat flow model and utilizes a thermal history sample treatment which masks the effects of chemical reactions.⁽⁵⁾ However, these chemical reactions significantly effect the temperature distribution in an oil-shale retort⁽⁶⁾ and form a key to understanding the behavior of thermal conductivity.

A key to unravelling some of the complexities in the thermal conductivity of oil shale lies in simultaneous parameter measurements. In this investigation thermal conductivity and electrical conductivity were measured simultaneously as a function of organic content, temperature and under stress levels simulating field conditions. These parameters were correlated and, as such, yielded much more useful results than thermal conductivity data alone. Some deviations from the major trends of previous work were observed.

SAMPLE PREPARATION

Mine-fresh rocks were obtained from the Paraho Oil Shale Development Corporation, Rifle, Colorado. Other samples were obtained from the Laramie Energy Research Center (LERC), Laramie, Wyoming. The five samples selected were analyzed by LERC using nuclear magnetic resonance. Their oil yield and sample number are given in table 1. Test specimens, cut perpendicular to the bedding plane, were carefully selected to insure that both the organic and the mineral matter were fairly evenly distributed and that the specimens contained no visible fractures. The polished specimens measured 2 inches in diameter and 3/4 inch thick. A groove, 0.100 inch deep, as shown in Fig. 7, was cut on each face of the specimen. Thermocouples in double bore ceramic tubes were inserted in the grooves, with the junction placed in direct contact with the shale. The thermocouples were fixed in place with Saureisen Cement.

* Supported under contract from the Laramie Energy Research Center of the U.S. ERDA.

EXPERIMENTAL PROCEDURE

Measurements were taken in a modified Dynatech⁽⁷⁾ TCFCM thermal conductivity apparatus. This apparatus is shown in Fig. 1a. The thermal conductivity measurement technique used is the "Comparative Method."⁽⁸⁾ This technique does not require (1) a diffusional model of heat flow, as does the transient line probe method; (2) it does not require drilling an extra thermocouple insertion hole into the oil shale sample; and (3) it does not require thermal history techniques to be utilized. The comparative method is similar to the standard Guarded Hotplate Technique,⁽⁸⁾ but is much faster and results in only a small sacrifice in accuracy. The modified apparatus was calibrated by measuring the thermal conductivity of Pyrex 7740 a number of times. The results showed a maximum deviation of 4 percent from published NBS results.

The oil-shale sample was sandwiched between two copper discs and the unit was sandwiched between two Pyrex 7740 reference samples as shown in Fig. 1b. The initial pressure was set using a Morehouse Ring Force gauge and power-screw apparatus shown in Fig. 1a. The pressure variation was determined by the variation on a ring force gauge dial indicator. The electrical resistance was determined by measuring the relative voltage drop across the shale between the two copper discs as compared to a reference resistor. A microvoltmeter was used to determine these voltages.

Complete runs were made on each sample at four average initial pressures shown in table 2. These runs were done in an air atmosphere at an approximate average heating rate of 65° F per hour. Experiments were started at ambient temperature and continued until the oil shales lost structural integrity--that is, to the temperature where the shale underwent complete structural collapse. Each specimen was heated in 45° F to 90° F increments per hour with a stack temperature gradient of 36° F to 54° F maintained across the test stack. When thermal steady state was attained, which required about 45 minutes per increment, stack temperatures, pressure, electrical resistivity, and time were recorded. The heaters were turned off during the pressure and electrical resistivity measurements to eliminate artifacts caused by heating and stray magnetic fields.

DATA ANALYSES

Experimental data were analyzed with a HP 2100 minicomputer. Thermal conductivity was computed according to equation

$$K_s = \frac{\lambda_s}{2\Delta T_s} \left\{ K_{TR} \frac{\Delta T_{TR}}{\lambda_{TR}} + K_{BR} \frac{\Delta T_{BR}}{\lambda_{BR}} \right\} \quad (1)$$

where the subscript "s" denotes the oil shale, "TR" the top reference, and "BR" the bottom reference. K is the thermal conductivity, ΔT the temperature drop, and λ the thermocouple to thermocouple spacing.

Electrical conductivity, stack temperatures, and pressure were also stored in a computer memory. These three sets of experimental data permitted us to compute three derived parameters as shown in Fig. 6: (1) one parameter coefficient of thermal expansion was computed using Equation 2

$$\beta = \frac{1}{\lambda_0} \frac{\Delta \lambda}{\Delta T} \quad (2)$$

where λ_0 is the original sample length, $\Delta \lambda$ the change in sample length over the temperature interval ΔT ; (2) the second derived parameter is the resistance ratio as it was computed according to Equation 3

$$R = \frac{V(T+\Delta T)}{V(T)} ; \quad (3)$$

(3) the third derived parameter, energy balance, is computed according to Equation 4. This parameter equals the ratio of the heat flowing into the top of the oil shale (Q_T) to the heat flowing out of the bottom of the oil-shale sample (Q_B).

$$\frac{Q_T}{Q_B} = \frac{k_{TR} \frac{\Delta T_{TR}}{L_{TR}}}{k_{BR} \frac{\Delta T_{BR}}{L_{BR}}} \quad (4)$$

The energy balance ratio (Q_T/Q_B) should equal unity at equilibrium, but deviates significantly from unity, as shown in Fig. 6, when heat is generated or absorbed during chemical reactions or physical transformations within the sample. The presence of carbonate minerals in an air ambient atmosphere caused chemical reactions to occur which seriously effected energy balance and temperature distributions. The thermal conductivity is not usually defined under nonequilibrium conditions such as those encountered over much of the temperature range we observed. What was measured was an effective thermal conductivity. Moreover, it can be shown that Equation 1 holds in the presence of heat generation within the sample as well as under equilibrium conditions.⁽⁹⁾ The effective thermal conductivity included the effect of the carbonate and kerogen decompositions, as well as the varve boundaries, cracks, and pores.

DISCUSSION OF EXPERIMENTAL DATA

The thermal conductivity versus temperature for four grades of oil shale at four different initial pressures, is shown in Fig. 2. The effect of pressure on the thermal conductivity becomes significant only at high temperatures. The pressures exerted by the oil shales on the press bar as a function of temperature are shown in Fig. 3. Even at low temperatures, these pressures were seen to increase. The pressures continued to increase until the specimens reached the structural transition temperature, at which point the specimens failed to sustain any stress and collapsed. The rapid decrease in pressure and eventual loss of structural integrity over a narrow temperature range was first reported by Tisot.⁽¹⁰⁾

The structural transition temperature also marks a significant change in the electrical and thermal transport parameters. Fig. 4 indicates that, just prior to the onset of structural yield, there is a change in the mechanism of the electrical conductivity. A measure of the nature of the electrical conduction mechanisms is the activation energy for electronic conduction, which is the slope of the electrical conductivity versus inverse temperature ($1/KT$) curve. The activation energy for electronic conduction may be obtained from Equation 5

$$E_a = \frac{T_2 - T_1}{KT_1 T_2} \ln \frac{\sigma_2}{\sigma_1} \quad (5)$$

where σ_2 and σ_1 are the conductivities measured at temperatures T_1 and T_2 . The electrical conductivity is plotted as a function of inverse temperature in Fig. 4. Electrical conductivity exhibits considerable variance at low temperatures, but all curves tend to coincide at temperatures approaching the structural transition temperature and above (Fig. 5). A least-squares fit to the data yields an activation energy for electrical conductivity of 1.8 eV at temperatures above the structural transition temperature. After the transition temperature, conductivity activation energy is reduced by a factor of almost two. The rapid rise in electrical conductivity is accompanied by a marked increase in the thermal conductivity. However, just prior to the structural transition temperature, the thermal conductivities attained a minimum (Fig. 2). After the transition temperature, the thermal conductivities increase. These increases in thermal conductivity are accompanied by a more rapid rise in the electrical conductivity, suggesting a possible electronic origin of the increase in thermal conductivity above the structural transition temperature.

One possible mechanism for the increase in the thermal conductivity at high temperature is a fundamental change in the heat conduction mechanism at the structural transition temperature. At low temperatures the shale is nonporous and conduction is mainly through solid-solid contact. The onset of chemical reactions in the oil shale, such as the decomposition of carbonates, alters the manner in which heat flows through the oil shale. Thus, in contrast to other workers,^(2,3) the experimental data show that the thermal conductivity often remains steady or increases with increasing temperature. Near the structural transition temperature, the oil shale, which was under uniaxial compression, began to consolidate. However, the oil shale could expand radially, and radially directed cracks and fissures could form. These structural flaws fill with air and gas, which have very low thermal conductivity, and therefore reduce the thermal conductivity of the oil shale. Above the structural transition temperature, oil shale begins to undergo structural failure along with chemical decomposition. Large numbers of pores which become increasingly filled with shale oil are formed (Fig. 7). This shale oil originates in those portions of the oil shale that begin to retort. As oil shale approaches retorting temperature, the relative contributions of solid-fluid and fluid-fluid heat transfer mechanisms increase and, at relatively low porosities, can dominate the thermal transport properties.⁽¹¹⁾

The increase of electrical and thermal conductivities at high temperatures, possibly caused by oil-filled pores, is supported by previous work which demonstrated that, for porous rocks, the electrical and thermal conductivities can be related to one another through a common parameter--porosity.⁽¹²⁾ In addition, shale oil at high temperatures appears to be highly electrically conductive. During one experiment, some shale oil seeped into a heater winding and caused a short circuit which damaged the heater. The high electrical conductivity of hot shale oil could cause difficulty in measuring oil-shale behavior at high temperatures since the shale oil could short-circuit thermocouples or other electrical transducers, unless they are properly insulated. It was also observed that the gray, retorted sections of the oil-shale samples used exhibited much higher resistivity than the unretorted sections.

The raw data exhibited considerable variations at particular temperatures. These variations are accentuated, and interparameter correlations highlighted, when the resistivity ratio, thermal expansion coefficient and energy balance at the temperature measurement data points are plotted for the various grades. A typical curve is shown in Fig. 6. The energy balance should be unity in equilibrium, but it begins to deviate substantially from unity as the shale undergoes decomposition reactions. These samples were heated in air and, hence, were subject to a number of carbonate decompositions beginning at about 195 F. Significant changes in the energy balance are accompanied by resistivity changes. The structural transition temperature is marked by rapid rises in the electrical and thermal conductivities.

SUMMARY AND CONCLUSIONS

The results from this investigation show that when oil shale is heated in air:

- (1) The thermal conductivity remains relatively constant up to the structural transition temperature (0.5 ± 0.15 Btu/ft-°F).
- (2) In a narrow temperature range around the structural transition temperature, thermal conductivity attains a minimum and then increases.
- (3) At temperatures above the structural transition temperature, all grades of shale exhibit the same activation energy for electronic conduction (1.8 eV).
- (4) The values of the electrical conductivity tend to coincide at temperatures above the structural transition temperature.
- (5) Below the structural transition temperature, the electrical conductivity is low and exhibits a spread in activation energies centered around 3.5 eV.

- (6) Simultaneous measurement of electrical conductivity, thermal conductivity, and pressure permits the computation of three derived parameters--the coefficient of thermal expansion, the energy balance ratio, and the resistance ratio.
- (7) The experimental data point to a common mechanism for the increase in thermal and electrical conductivities at temperatures above the structural transition temperature. This mechanism is the filling of pores with conductive shale oil.

The data reported here can be used to develop an improved mathematical model of oil-shale retorting. The electrical and pressure data can be used to develop sensors which predict the onset of structural failure and kerogen decomposition.

ACKNOWLEDGMENTS

The authors acknowledge the helpful criticism, friendly advice and experimental intuition provided by P. R. Tisot who did much to assist in experimental design, sample selection and data analysis. The authors thank Howard Jensen and John Duvall of the Laramie Energy Research Center, Laramie, Wyoming, for furnishing guidance during the course of the work. The authors thank Tom Meals, Philip Milling and Robert Wiff for support in various phases of this work.

BIBLIOGRAPHY

1. Cameron Engineers, "Synthetic Fuels Data Book," June 1975.
2. Prats, M. and O'Brien, S., "Thermal Conductivity and Diffusivity of Green River Oil Shale," JPT, Jan. 1975, pp. 97-106.
3. Tihen, S., Carpenter, H., and Sohns, H., "Thermal Conductivity and Thermal Diffusivity of Green River Oil Shale," NBS Special Publication, 1968.
4. Cook, E. W., "Thermal Analysis of Oil Shales," Quarterly of Colorado School of Mines, vol. 65, No. 4, Oct. 1970, p. 133.
5. Woodside, W., and Messmer, J., "Thermal Conductivity of Porous Media II Consolidated Rocks," J. Appl. Phys., 32, 9, 1961, p. 1699.
6. Fausett, D., "A Mathematical Model of an Oil Shale Retort," Quarterly of Colorado School of Mines, July 1975.
7. Reference to a brand name does not imply endorsement of the product by the investigators or the Laramie Energy Research Center of the U.S. ERDA.
8. Powell, R., "Thermal Comparator Methods," in Thermal Conductivity, vol. 2, R. Tye, ed., Academic Press, 1968.
9. DuBow, J., Nottenburg, R., and Collins, G., "Thermal and Electrical Conductivity of Green River Oil Shale," Final Report, June 1976.
10. Tisot, P. R., "Alterations in Structure and Physical Properties of Green River Oil Shale by Thermal Treatment," J. Chem. Eng. Data, v. 12, No. 3, 1967, p. 405.
11. Huang, J. N., "Effective Thermal Conductivity of Porous Rocks," J. Geophys. Res., vol. 76, No. 26, p. 6420, 1971.
12. Hust, J. and Berg, J., "Thermal and Electrical Conductivities of Sandstone Rocks and Ocean Sediments," Geophys., vol. 33, No. 3, 1968.

<u>Sample</u>	<u>Grade (gpt)</u>
AAII top	21.6
AAII bottom	25.1
AA2 top	29.6
AA2 bottom	32.2
AA8 top	47.9

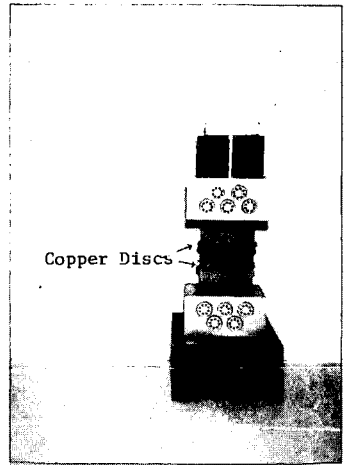
Table 1 Notation For Oil Shale Grades Reported in Subsequent Figures

<u>Condition</u>	<u>Uniaxial Pressure Applied to Sample (psi)</u>
1	120
2	310
3	460
4	600

Table 2 Notation used in Figures To Designate the Four Conditions of Pressure applied to the Sample



a



b

Fig. 1: a) Apparatus b) Test Stack

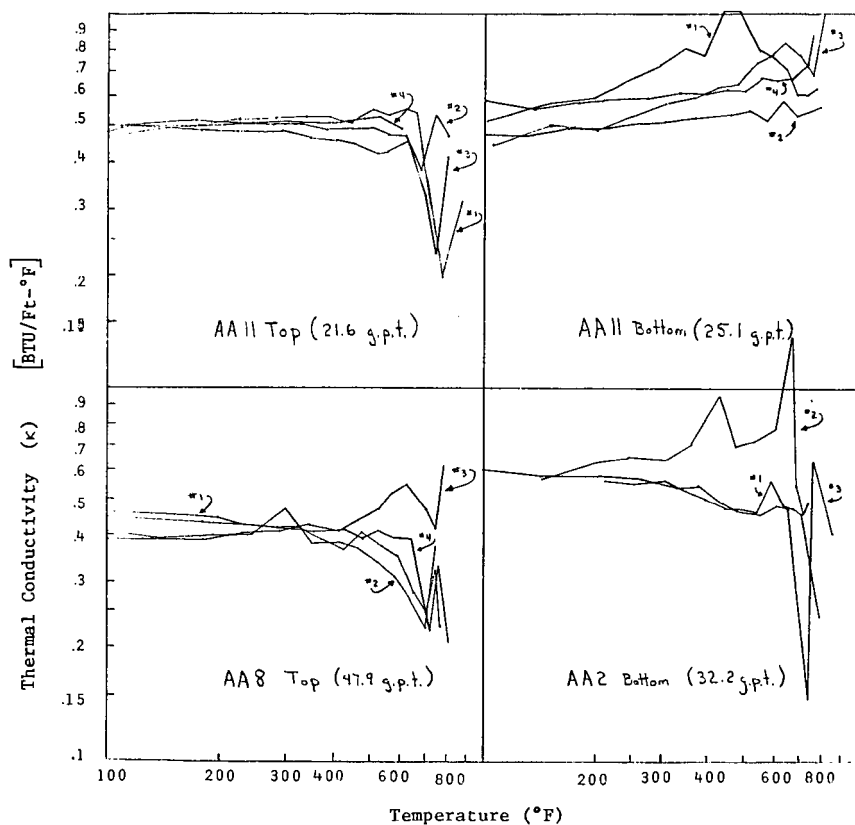


Fig 2: Thermal Conductivity versus Temperature for four selected grades of oil shale at four different pressures

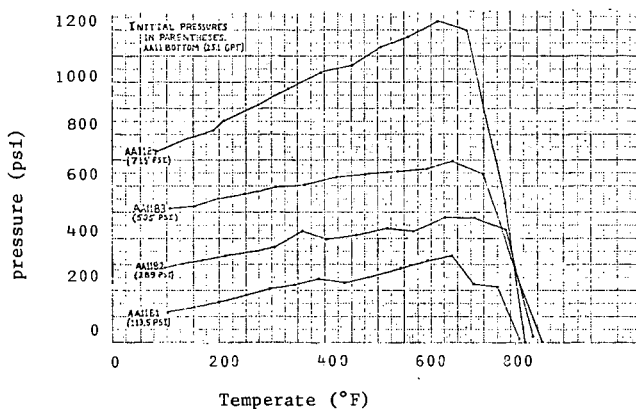


Fig. 3. Variation of Pressure with Temperature for Samples
AA 11 B (25.1 g. p. t.)

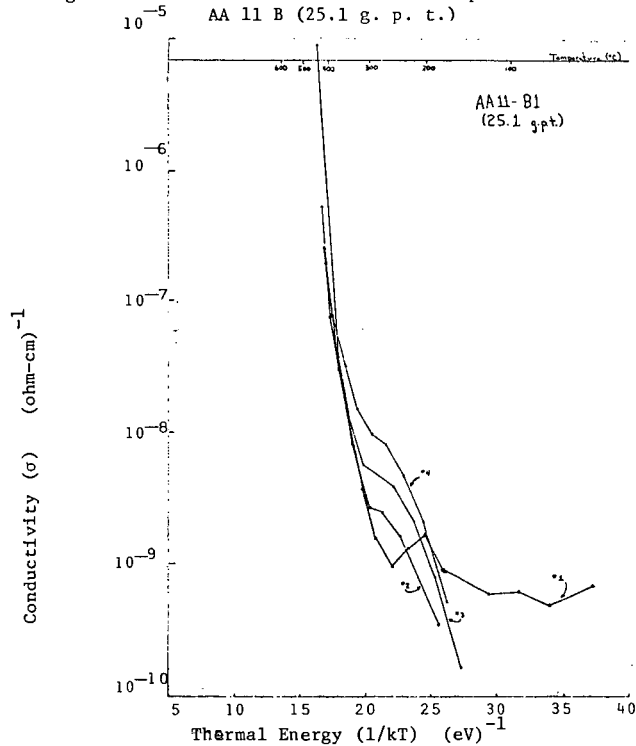


Fig. 4: Electrical Conductivity versus temperature with pressure as a parameter

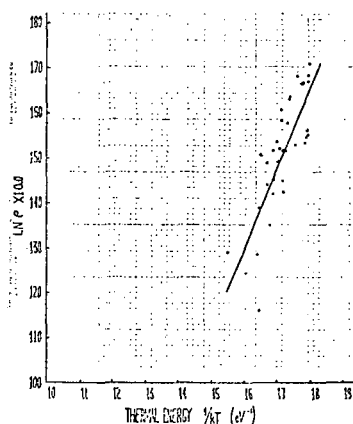


Fig. 5. Plot of least squares fit of resistivity vs. temperature for many oil shale samples which exhibit an activation energy of 1.8 eV.

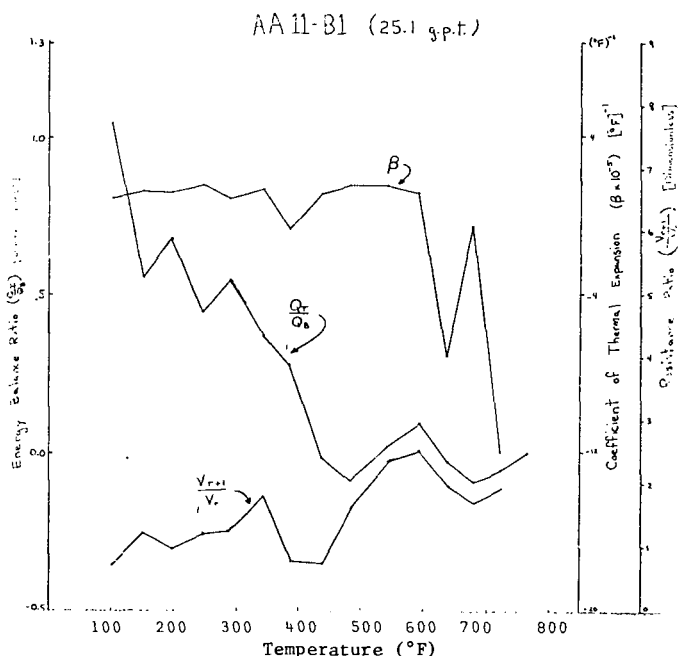


Fig. 6 Derived parameters: energy balance ratio, resistance ratio, and coefficient of thermal expansion versus temperature (°F)

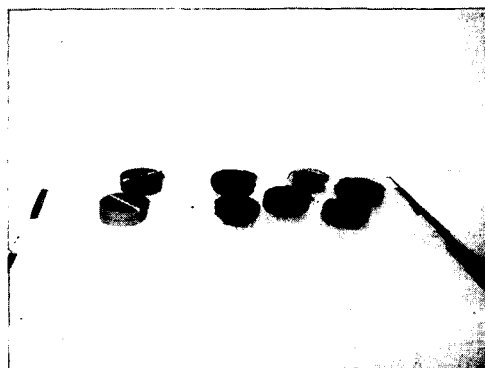


Fig. 7 Samples before and after experiment